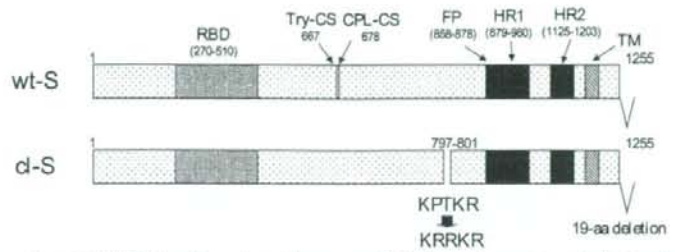

FIG. 1. Schematic illustration of SARS-CoV wt-S protein and its mutant (cl-S). S proteins are shown in the box, in which the RBD, putative fusion peptide (FP), two HRs, and transmembrane region (TM) are indicated. Cleavage sites by trypsin (Try-CS) and CPL (CPL-CS) are also shown. Amino acid positions 798 and 799 are changed into arginine to make the recognition sequence of furin-like protease, KRRKR. Nineteen C-terminal amino acids (aa) are deleted for the efficient pseudotype formation of VSV.

cleavage and fusogenic activation of SARS-CoV S protein are a critical step for virus entry into cells.

The preceding observations led us to postulate that SARS-CoV with cl-S protein that induces cell-to-cell fusion in the absence of proteases is able to enter cells directly from the cell surface, being similar to the cell entry of MHV with cl-S protein (16, 28). To explore this possibility, we have made a cleavage mutant of the SARS-CoV S protein by introducing the recognition sequence of furin-like protease, produced pseudotyped vesicular stomatitis virus (VSV) bearing this S protein, and analyzed whether cl-S protein facilitates direct viral entry from the cell surface.

We have chosen two different sites of S protein to introduce the furin recognition sequence (FRS) (RXR/KR; X indicates any amino acid residue [11]), one at positions 663 to 667 and the other at 798 to 801, since both contain a few endogenous basic amino acids and need not be drastically mutated to introduce FRS. The former corresponds to the site cleaved by trypsin (22) and also to the site of the MHV S protein which is cleaved during biosynthesis (36); however, insertion of FRS in this region failed to produce cleaved and fusogenic S protein in our system, being different from a previous report by Follis et al. (14). Thus, we introduced the FRS into a second region at positions 798 to 801. The mutated S protein was revealed to be fusogenic and was also cleaved by endogenous proteases, most probably by furin. In this study, we have analyzed the relationship of cleavability and fusogenicity of S protein as well as the cell entry pathway of the pseudotype VSV bearing the cl-S protein (VSV/cl-S) with a mutation at amino acid positions 798 to 801.

FRS was introduced at amino acid positions 798 to 801 in SARS-CoV S protein by an overlapping PCR method (14), and the resultant S protein was designated cl-S. Nineteen C-terminal amino acids were deleted for the efficient formation of pseudotype VSV, as described by Fukushi et al. (15). The mutated cDNA, as well as the cDNA for wild-type S (wt-S) protein lacking the 19 C-terminal amino acid residues, was cloned into a pCAG vector, and the nucleotide sequence was confirmed by DNA sequencing using BigDye Terminator version 3.1 and a 3130xl genetic analyzer (Applied Biosystems, Foster, CA). Figure 1 shows a schematic illustration of these S proteins.

The expression plasmids pCAG/cl-S and pCAG/wt-S, encoding SARS-CoV cl-S and SARS-CoV wt-S proteins, respectively, were transfected into HeLa cells and HeLa-ACE2 cells by using FuGENE6 (Roche Diagnostics, Mannheim, Germany), and those cells were incubated for 48 h after transfection. HeLa-ACE2 cells that constitutively express ACE2 were established from HeLa cells, following the transfection of a plasmid to express ACE2. The cells cultured for 48 h were also treated with 20 μg/ml of trypsin at room temperature for 5 min and further cultured at 37°C for 2 h to check cell fusion. As shown in Fig. 2A, large syncytia were visible on the HeLa-ACE2 cells transfected with pCAG/cl-S without trypsin treatment, whereas there was no apparent syncytium formation on the cells transfected with pCAG/wt-S. Treatment with trypsin induced fusion of the cells expressing wt-S protein. On the other hand, neither of those S proteins could induce cell-to-cell fusion on HeLa cells, even when they were treated by trypsin. These results strongly indicated that the cleavage of the S protein at amino acid position 798 converted its protease-dependent fusion phenotype to a protease-independent one and that ACE2 is crucial for the induction of cell-to-cell fusion. We then confirmed the cleavage of the S protein in those cells by Western blot analysis using anti-S2 rabbit serum no. 557 (Imgenex, San Diego, CA). Cells treated or untreated with trypsin were lysed with lysis buffer (10% glycerol, 1% Triton X-100, 135 mM NaCl) 5 min after treatment, and cell lysates were subjected to Western blot analysis. As shown in Fig. 2B, an S2 fragment with a molecular mass of 70 kDa was detected in the cell lysates prepared from pCAG/cl-S-transfected HeLa-ACE2 cells but not in the lysate of cells transfected with pCAG/wt-S (Fig. 2B). The 70-kDa protein found in cells transfected with pCAG/cl-S seems likely to correspond to the S2 fragment cleaved at the site where mutations recognized by furin-like protease are inserted, since its putative size was calculated to be approximately 68 kDa. It was also found that a proportion of cl-S protein expressed on HeLa-ACE2 cells was cleaved into a 100-kDa protein from a 240-kDa uncleaved form of S protein by trypsin treatment. The appearance of this 100-kDa protein in the lysates of trypsin-treated cells could result from the cleavage at amino acid position 667 (22), consistent with previous reports, and this subunit has been suggested to be involved in an S protein-mediated fusion (27, 32). Accordingly, cell fusion induction by trypsin of wt-S protein-expressing cells shown in the present study may be due to the

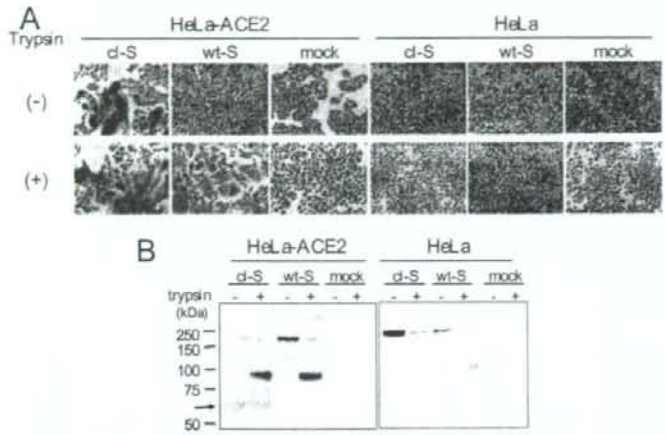

FIG. 2. Fusion formation and cleavability of cl-S and wt-S proteins transiently expressed in cells with and without ACE2 expression. (A) HeLa-ACE2 and HeLa cells were transfected with pCAG plasmid containing cl-S or wt-S proteins or were mock transfected (mock) by using FuGENE6 and were incubated for 48 h. Then, cells were treated (+) or untreated (−) with 20 μg/ml of trypsin at room temperature for 5 min and further incubated in DMEM containing 5% FBS at 37°C for 2 h. Then, formalin-fixed cells were stained with crystal violet. (B) Expression of the S2 subunit in cells transfected with S protein expression plasmids. Cells treated as described above were lysed before (−) or after (+) trypsin treatment and analyzed by Western blotting using anti-S2 antiserum (no. 557; Imgenex). Arrow indicates the cl-S2 subunit, as judged by its molecular size.

presence of 100 kDa of S2 protein (Fig. 2B). Also, the slightly elevated syncytium formation by trypsin treatment of the cells expressing cl-S protein 48 h after transfection (Fig. 2A, compare HeLa-ACE2 cells expressing cl-S protein and treated with trypsin to similar cells without trypsin treatment) could be attributed to a 100-kDa protein that arose after trypsin treatment. When cl-S protein was expressed in HeLa cells deleting ACE2, cleavage products were not detected, resulting in the absence of cell-to-cell fusion. Treatment of HeLa cells expressing wt-S or cl-S proteins with trypsin facilitated the cleavage of 240 kDa into 100 kDa, which was similar to the type of cleavage observed in HeLa-ACE2 cells; however, no fusion was detected, which indicated to us that ACE2 is crucial for the induction of cell-to-cell fusion. These results suggest that cl-S protein with a 70-kDa S2 subunit can induce fusion in a protease-independent manner.

Recently, Bosch et al. reported that SARS-CoV S proteins were cleaved by CPL at amino acid 678, resulting in a ca. 70-kDa S2 subunit (5), while the cl-S protein cleaved at position 798 shown in this study also resulted in a 60- to 70-kDa S2 subunit, even if the cleavage site was about 120 amino acids apart. This coincidence of the molecular mass of two different S2 subunits could come from the difference of S protein structure used in each experiment. We used full-length S, deleting 19 C-terminal amino acids, while S protein utilized by Bosch et al. was the soluble form of S protein, deleting transmembrane, and cytoplasmic domains consisted of ca. 60 amino acids (5). The full-length S2 subunit cleaved by CPL in SARS-CoV-infected cells would be ca. 100 kDa, similar to the S2 subunit cleaved by trypsin, because cleavage sites of those two proteases are closely located and only 11 amino acids apart (5, 22).

To evaluate the significance of the cleavage of the S protein to the entry pathway of SARS-CoV, pseudotyped VSV/cl-S or VSV/wt-S protein was produced as described previously (15, 26). In brief, expression plasmids for cl-S or wt-S protein were transfected to 293T cells, and those cells were infected with VSV bearing the glycoprotein (G), VSVΔG*G/SEAP, or VSVΔG*G/GFP, at 36 h after transfection. VSVΔG*G/SEAP and VSVΔG*G/GFP have a secretary alkaline phosphatase (SEAP) gene and the green fluorescence protein (GFP) gene in place of the VSV viral G gene, respectively. To confirm the S protein on the pseudotype viruses released in the culture supernatants, the supernatant was collected at 24 h after infection, and pseudotyped VSV was concentrated by ultracentrifugation at 45,000 rpm for 2 h at 4°C using an SW50.1 rotor (Beckman, Fullerton, CA). The resultant pellets were dissolved in phosphate-buffered saline, pH 7.2, and analyzed by Western blotting after sodium dodecyl sulfate-polyacrylamide gel electrophoresis. To detect S1 and S2 subunits, we used anti-S1 no. 20 (epitope, 20 to 35) and anti-S2 no. 1125 (epitope, 1125 to 1140) produced by the immunization of a chicken with synthetic peptides. As shown in Fig. 3A, a ca. 150-kDa protein and a 240-kDa protein was detected on pseudotyped VSV/cl-S by anti-S1 antibodies, while a ca. 70-kDa as well as a 240-kDa protein was detected by S2 subunit-specific antibodies. On the other hand, only the 240-kDa protein was seen on the pseudotype VSV/wt-S by both antibodies. The 150-kDa and 70-kDa proteins detected on pseudotype VSV/cl-S by anti-S1 and S2 antibodies, respectively, were thought to be cleavage products from their antigenicity and sizes. These results indicate that VSV pseudotypes with cl-S or wt-S protein were successfully formed, although the former is a mixture of pseudotypes with cl-S and uncleaved S protein (Fig. 3A). To obtain a preparation containing a higher proportion of pseudotype with cl-S protein, we expressed furin and ACE2 in 293T cells transfected with pCAG/cl-S because the production of a 70-kDa S2 subunit during synthesis was observed only in the presence of ACE2 (Fig. 2B). However, this

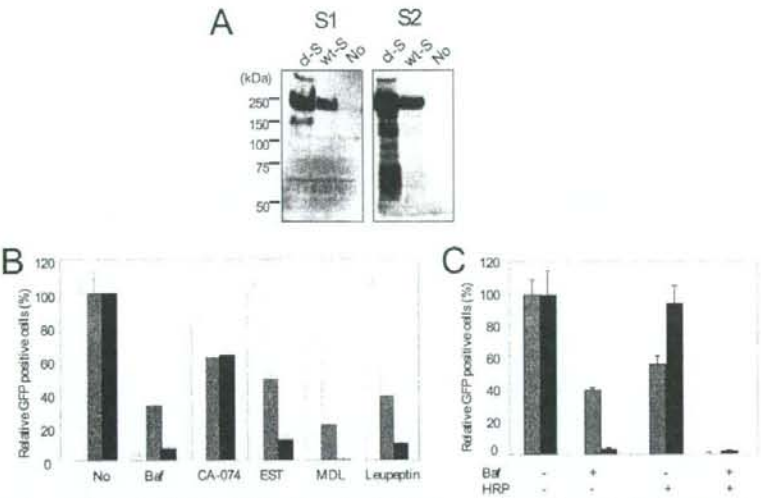

FIG. 3. Analysis using pseudotype VSV/cl-S or VSV/wt-S protein. (A) The incorporation of S protein into the pseudotype VSV. Pseudotype VSV was prepared by transfection of expression plasmids harboring the cl-S gene, the wt-S gene, or no gene and infection of VSVΔG*G. The pseudotypes in the culture fluids were concentrated by spinning at 45,000 rpm for 2 h using the SW50.1 rotor of a Beckman ultracentrifuge. The resultant pellets were dissolved in lysis buffer and analyzed by Western blot analysis using chicken antisera against S1 and S2 subunits (anti-S1 no. 20 and anti-S2 no. 1125, respectively). (B) Effect of Baf, protease inhibitors CA-074, EST, MDL, or leupeptin on the infection of VSV/G (white column), VSV/cl-S (gray column), or VSV/wt-S (black column) protein. HeLa-ACE2 cells prepared in 96-well plates were treated with those reagents at 37°C for 1 h, and ca. 500 PFU/50 μl of pseudotype VSVs were challenged. The infection was evaluated by measuring the number of GFP gene-positive cells in the wells at 24 h after infection as determined by Keyence fluorescence microscopy. (C) Blockade of pseudotype VSV infection by HRP. HeLa-ACE2 cells prepared in 96-well plates were treated with either Baf and/or HRP (5 μM) for 30 min at 37°C, infected with pseudotype VSVs that express GFP, adsorbed at 4°C for 1 h, and then incubated in the presence of Baf and/or HRP at 37°C for 24 h. The infection was evaluated as described above.

treatment did not increase the amount of cl-S proteins on the pseudotypes (data not shown).

We then examined the cell entry pathway of the viruses with cl-S and uncleaved SARS-CoV S proteins by using the above-mentioned preparation of two different pseudotype VSVs. To see whether the virus with cl-S protein bypassed an endosomal pathway, we evaluated the effect on the virus infection of the lysosomotropic agent bafilomycin A1 (Baf) in HeLa-ACE2 cells. The cells seeded at a concentration of 2×10^4 cells per well in a 96-well culture plate (Smilon, Tokyo, Japan) the day before infection were incubated in Dulbecco's minimum essential medium (DMEM; Nissui, Tokyo, Japan) containing 5% fetal bovine serum (FBS; Sigma) and 100 nM Baf (Sigma) for 1 h at 37°C before infection. Then, ca. 500 infectious units of GFP gene-positive pseudotype VSV/cl-S, VSV/wt-S, or VSV/G was inoculated and incubated at 37°C for 1 h. Those cells were further incubated for 23 h in DMEM plus 5% FBS containing 100 nM Baf. GFP gene-positive cells were photographed by Keyence fluorescence microscopy (Keyence Corporation, Osaka, Japan), and cell numbers were calculated by using the image measurement and analyzing software VH-H1A5 version 2.6 (Keyence). As shown in Fig. 3B, the infection by VSV/wt-S was reduced by more than 90% by Baf treatment, similar to the suppression seen with VSV/G infection, which takes the endosomal pathway, while the suppression of VSV/cl-S infection was ca. 60%. This finding indicated that a proportion of VSV/cl-S infection was not affected by low pH in the endosome, which suggested that pseudotypes with cl-S protein do not take the endosomal pathway. About 60% of the reduction in infection of VSV/cl-S could be accounted for by the pseudotypes bearing uncleaved S protein, which was contaminated in the pseudotype with cl-S protein, as shown in Fig. 3A. We then examined whether the infection of pseudotypes is affected by treatment with protease inhibitors in a manner similar to that seen with SARS-CoV infection (33). Cells were treated with DMEM containing 100 μM of CPL inhibitor MDL (Sigma), 50 μM of CPL inhibitor EST (Carbiochem, Darmstadt, Germany), 200 μM of cathepsin B inhibitor CA-074 (Sigma), or 50 μM of cysteine protease inhibitor leupeptin (Roche Diagnostics) in a manner similar to that with Baf treatment and then infected with pseudotype viruses. GFP gene-positive cells were calculated as described above. Infection with the pseudotype bearing wt-S protein was heavily blocked by MDL, EST, and leupeptin, while pseudotypes with cl-S protein infection were partially inhibited (Fig. 3B), which indicated that VSV/wt-S requires CPL for its infection, while VSV/cl-S does not require CPL. A fraction of pseudotypes with cl-S protein sensitive to protease inhibitor treatment is also explained by the contamination of a pseudotype bearing uncleaved S protein. These results collectively suggest that VSV/cl-S could bypass the endosomal pathway in which S protein activation was induced by CPL and, thus, that VSV/cl-S most likely enters target cells directly from the cell surface.

To further confirm that VSV/cl-S enters directly from the cell surface, we utilized a heptad repeat peptide (HRP) that was recently shown to efficiently block SARS-CoV infection from the cell surface but not the infection via the endosomal pathway (38). HeLa-ACE2 cells were treated with a final concentration of 100 nM of Baf and/or 5 μM of HRP-SR9, a peptide of 35 amino acids that corresponds to positions 1151 to 1185 of the SARS-CoV S protein (38), for 30 min at 37°C. Then, pseudotype VSVs were allowed to attach to cells at 4°C for 1 h in the presence of those agents. Then, cells were cultured at 37°C for 24 h in their presence, and the number of GFP gene-positive cells was calculated. As shown in Fig. 3C, Baf treatment alone thoroughly blocked infection with VSV/wt-S and that of VSV/cl-S by 40%, which seemed to indicate that some population of VSV/cl-S could bypass the endosomal pathway as shown in Fig. 3B. When treated with HRP, infection with VSV/wt-S was not at all blocked, which was similar to the results obtained previously (38), while infection with VSV/cl-S was partially blocked. The fraction of virus inhibited by HRP treatment may represent the VSV/cl-S. Furthermore, when treated with Baf and HRP, infection with VSV/cl-S was blocked almost completely, which suggested that the infection of Baf-resistant VSV/cl-S was blocked by HRP treatment. Another HRP (SR9EK1), previously shown to not prevent cell surface entry (38), failed to inhibit VSV/cl-S infection (data not shown). These results suggest that VSV/cl-S enters directly from the cell surface.

Two different pathways for cell entry are known for enveloped viruses, one from the cell surface and the other via an endosome (12). HIV and influenza virus are representative of the former and latter, respectively. Following binding to its receptor/coreceptor, gp160 of HIV is fusogenically activated, and fusion of the viral envelope and plasma membrane takes place, which facilitates the entry of the virus directly from the cell surface. In contrast, activation by hemagglutinin of influenza virus requires a low pH environment in the endosome to which virions are trafficked, following binding to its receptor. A strain of murine CoV, MHV-JHM, is believed to enter cells from the cell surface (16), while another strain, namely, MHV-A59, uses an endosomal pathway for entry due to its similarity to the entry mechanism of influenza virus (13). Although SARS-CoV takes an endosomal pathway, the molecular mechanism of entry is quite different from that of MHV-A59 or influenza virus. SARS-CoV S protein activation is not induced under a low pH environment but by proteolytic cleavage by CPL in the endosome that provides a low pH environment, which is optimal for CPL activity (5, 33). This entry mechanism is unique, though Ebola virus was initially shown to enter into cells in a similar fashion (9). Based on these molecular events of SARS-CoV infection, it can be postulated that SARS-CoV bearing a cl-S protein with fusion activity is able to enter cells directly from the cell surface, such as HIV and MHV-JHM do. The present study showed that cl-S protein along with the cell fusion activity of SARS-CoV facilitated viral entry into cells directly from the cell surface and strengthened the premise concerning the cell entry mechanism of SARS-CoV, as proposed by previous findings from different laboratories (27, 32, 33).

In the present study, we designed a mutant S protein to be cleaved during its maturation at the 798 amino acid position by inserting a recognition site for the furin-like protease. The detection of a 70-kDa fragment by anti-S2 antibody in Western blot analysis suggests that cleavage takes place at an expected position. Follis et al. produced a mutant with a cleavage site at amino acid position 667 (14). An S2 subunit of this mutant S protein was shown to be ca. 100 kDa and fusogenic, although insertion of extra amino acids in a newly appearing cleavage site is required for enhanced fusogenicity (14). We also produced and expressed the S protein without an extra amino acid insertion, as reported by Follis et al. (14), although it failed to induce cell-to-cell fusion in the absence of trypsin but successfully induced fusion when treated with trypsin, similar to the wt-S protein (data not shown). In our system, S protein with a cleavage site at amino acid 798 is only an S protein competent in the induction of cell-to-cell fusion without trypsin treatment.

It is clear that there is no stringency in the cleavage site of the SARS-CoV S protein for the fusion activity. Cleavage of the S protein by trypsin and CPL resulted in the fusion activity (5, 27, 32), even if the cleavage site was slightly different (5, 22). Also, our present study showed that cleavage at 120 amino acids downstream compared with the sites of trypsin and CPL conferred the fusion activity to the S2 protein. This is a unique feature of CoV S protein that was not found in the envelope protein of other viruses having a class I fusion protein, like HIV or influenza virus.

The finding that cl-S2 cleaved at position 798 has fusion activity implies that this molecule has a fusion peptide together with two different heptide repeats (HRs), motifs critical for fusion activity of class I fusion protein of the virus. This suggests that the fusion peptide on SARS-CoV S protein would locate downstream of amino acid position 798. Although there are controversial reports on the localization of a fusion peptide in SARS-CoV S protein, present study suggests that the fusion peptide locates immediately upstream of the HR1 (18) rather than in the 770 to 788 region (30), because this region is located outside the fusogenic 70-kDa S2 subunit produced by cl-S protein expression.

We reported that SARS-CoV infection was enhanced in cultured cells in the presence of proteases, such as trypsin and elastase, and that this enhancement was facilitated by virus entry from the cell surface (27). Elastase is a major protease produced by neutrophils during lung inflammation and may be relevant to the high growth of SARS-CoV in the lung, a major target organ (20). Based on these findings, we have established an exacerbated fatal pneumonia of mice with high pathogenic similarity to human SARS by the coinfection of SARS-CoV and nonpathogenic respiratory bacteria that stimulates elastase secretion (1). Severe pneumonia of mice was attributed to an enhanced SARS-CoV infection in the lung that could be facilitated by the elastase (1). We have not evaluated yet whether this enhanced infection is due to the cell surface infection. If this is the case, HRP may be a good candidate for a therapeutic tool, since HRP efficiently blocks SARS-CoV infection from the cell surface, as shown in the present and previous studies (38).

Most MHV strains induce cell-to-cell fusion in infected cells, yet a highly hepatopathogenic strain, MHV-2, fails to induce fusion (41). MHV-2 shares a common feature with SARS-CoV in terms of its S protein. MHV-2 was revealed to enter cells in

a fashion highly similar to that of SARS-CoV, which is dependent on the proteases in the endosomal compartment having a low pH environment (28). A mutant virus with fusogenic S protein was isolated from wild-type MHV-2 bearing uncleaved S protein, although isolation was extremely low in efficiency, ca. 1 mutant out of half a million to 1 million (41). This could suggest the possibility that SARS-CoV with fusogenic cl-S protein exists among a large number of viruses with uncleaved S protein. It is of interest to see the effects of SARS-CoV with a cl-S protein in terms of cell entry mechanisms as well as in pathogenesis for animals.

We thank Miyuki Kawase for her excellent technical assistance, Makoto Ujike for helpful discussions, and Hiroki Nishikawa and Nobutaka Fujii for providing HRP. We also thank Sarah Connolly for editing the manuscripts and for valuable comments.

This work was supported by grants from the Ministry of Education, Culture, Science, and Technology and from the Ministry of Health, Labor, and Welfare.

REFERENCES

1. **Ami, Y., N. Nagata, K. Shirato, R. Watanabe, N. Iwata, K. Nakagaki, S. Fukushi, M. Saijo, S. Morikawa, and F. Taguchi.** 2008. Co-infection of respiratory bacterium with SARS coronavirus induces an exacerbated pneumonia in mice. Microbiol. Immunol. **52:**118–127.
2. **Babcock, G. J., D. J. Esshaki, W. D. Thomas, Jr., and D. M. Ambrosino.** 2004. Amino acids 270 to 510 of the severe acute respiratory syndrome coronavirus spike protein are required for interaction with receptor. J. Virol. **78:**4552–4560.
3. **Bergeron, E., M. J. Vincent, L. Wickham, J. Hamelin, A. Basak, S. T. Nichol, M. Chretien, and N. G. Seidah.** 2005. Implication of proprotein convertases in the processing and spread of severe acute respiratory syndrome coronavirus. Biochem. Biophys. Res. Commun. **326:**554–563.
4. **Bonavia, A., B. D. Zelus, D. E. Wentworth, P. J. Talbot, and K. V. Holmes.** 2003. Identification of a receptor-binding domain of the spike glycoprotein of human coronavirus HCoV-229E. J. Virol. **77:**2530–2538.
5. **Bosch, B. J., W. Bartelink, and P. J. M. Rottier.** 2008. Cathepsin L functionally cleaves the SARS-CoV class-I fusion protein upstream of rather than adjacent to the fusion peptide. J. Virol. **82:**8887–8890.
6. **Bosch, B. J., B. E. Martina, R. van der Zee, J. Lepault, B. J. Haijema, C. Versluis, A. J. Heck, R. de Groot, A. D. Osterhaus, and P. J. Rottier.** 2004. Severe acute respiratory syndrome coronavirus (SARS-CoV) infection inhibition using spike protein heptad repeat-derived peptides. Proc. Natl. Acad. Sci. USA **101:**8455–8460.
7. **Bosch, B. J., R. van der Zee, C. A. de Haan, and P. J. Rottier.** 2003. The coronavirus spike protein is a class I virus fusion protein: structural and functional characterization of the fusion core complex. J. Virol. **77:**8801–8811.
8. **Chan, D. C., and P. S. Kim.** 1998. HIV entry and its inhibition. Cell **93:**681–684.
9. **Chandran, K., N. J. Sullivan, U. Felbor, S. P. Whelan, and J. M. Cunningham.** 2005. Endosomal proteolysis of the Ebola virus glycoprotein is necessary for infection. Science **308:**1643–1645.
10. **Delmas, B., J. Gelfi, E. Kut, H. Sjostrom, O. Noren, and H. Laude.** 1994. Determinants essential for the transmissible gastroenteritis virus-receptor interaction reside within a domain of aminopeptidase-N that is distinct from the enzymatic site. J. Virol. **68:**5216–5224.
11. **Duckert, P., S. Brunak, and N. Blom.** 2004. Prediction of proprotein convertase cleavage sites. Protein Eng. Des. Sel. **17:**107–112.
12. **Eckert, D. M., and P. S. Kim.** 2001. Mechanisms of viral membrane fusion and its inhibition. Annu. Rev. Biochem. **70:**777–810.
13. **Eifart, P., K. Ludwig, C. Bottcher, C. A. de Haan, P. J. Rottier, T. Korte, and A. Herrmann.** 2007. Role of endocytosis and low pH in murine hepatitis virus strain A59 cell entry. J. Virol. **81:**10758–10768.
14. **Follis, K. E., J. York, and J. H. Nunberg.** 2006. Furin cleavage of the SARS coronavirus spike glycoprotein enhances cell-cell fusion but does not affect virion entry. Virology **350:**358–369.
15. **Fukushi, S., T. Mizutani, M. Saijo, S. Matsuyama, N. Miyajima, F. Taguchi, S. Itamura, I. Kurane, and S. Morikawa.** 2005. Vesicular stomatitis virus pseudotyped with severe acute respiratory syndrome coronavirus spike protein. J. Gen. Virol. **86:**2269–2274.
16. **Gallagher, T. M., C. Escarmis, and M. J. Buchmeier.** 1991. Alteration of the pH dependence of coronavirus-induced cell fusion: effect of mutations in the spike glycoprotein. J. Virol. **65:**1916–1928.
17. **Garwes, D. J., and D. H. Pocock.** 1975. The polypeptide structure of transmissible gastroenteritis virus. J. Gen. Virol. **29:**25–34.
18. **Guillén, J., A. J. Perez-Berna, M. R. Moreno, and J. Villalain.** 2005. Identification of the membrane-active regions of the severe acute respiratory syndrome coronavirus spike membrane glycoprotein using a 16/18-mer peptide scan: implications for the viral fusion mechanism. J. Virol. **79:**1743–1752.
19. **Hofmann, H., G. Simmons, A. J. Rennekamp, C. Chaipan, T. Gramberg, E. Heck, M. Geier, A. Wegele, A. Marzi, P. Bates, and S. Pöhlmann.** 2006. Highly conserved regions within the spike proteins of human coronaviruses 229E and NL63 determine recognition of their respective cellular receptors. J. Virol. **80:**8639–8652.
20. **Kawabata, K., T. Hagio, and S. Matsuoka.** 2002. The role of neutrophil elastase in acute lung injury. Eur. J. Pharmacol. **451:**1–10.
21. **Kubo, H., Y. K. Yamada, and F. Taguchi.** 1994. Localization of neutralizing epitopes and the receptor-binding site within the amino-terminal 330 amino acids of the murine coronavirus spike protein. J. Virol. **68:**5403–5410.
22. **Li, F., M. Berardi, W. Li, M. Farzan, P. R. Dormitzer, and S. C. Harrison.** 2006. Conformational states of the severe acute respiratory syndrome coronavirus spike protein ectodomain. J. Virol. **80:**6794–6800.
23. **Li, W., M. J. Moore, N. Vasilieva, J. Sui, S. K. Wong, M. A. Berne, M. Somasundaran, J. L. Sullivan, K. Luzuriaga, T. C. Greenough, H. Choe, and M. Farzan.** 2003. Angiotensin-converting enzyme 2 is a functional receptor for the SARS coronavirus. Nature **426:**450–454.
24. **Luo, Z., and S. R. Weiss.** 1998. Roles in cell-to-cell fusion of two conserved hydrophobic regions in the murine coronavirus spike protein. Virology **244:**483–494.
25. **Marra, M. A., S. J. Jones, C. R. Astell, R. A. Holt, A. Brooks-Wilson, Y. S. Butterfield, J. Khattra, J. K. Asano, S. A. Barber, S. Y. Chan, A. Cloutier, S. M. Coughlin, D. Freeman, N. Girn, O. L. Griffith, S. R. Leach, M. Mayo, H. McDonald, S. B. Montgomery, P. K. Pandoh, A. S. Petrescu, A. G. Robertson, J. E. Schein, A. Siddiqui, D. E. Smailus, J. M. Stott, G. S. Yang, F. Plummer, A. Andonov, H. Artsob, N. Bastien, K. Bernard, T. F. Booth, D. Bowness, M. Czub, M. Drebot, L. Fernando, R. Flick, M. Garbutt, M. Gray, A. Grolla, S. Jones, H. Feldmann, A. Meyers, A. Kabani, Y. Li, S. Normand, U. Stroher, G. A. Tipples, S. Tyler, R. Vogrig, D. Ward, B. Watson, R. C. Brunham, M. Krajden, M. Petric, D. M. Skowronski, C. Upton, and R. L. Roper.** 2003. The genome sequence of the SARS-associated coronavirus. Science **300:**1399–1404.
26. **Matsuura, Y., H. Tani, K. Suzuki, T. Kimura-Someya, R. Suzuki, H. Aizaki, K. Ishii, K. Moriishi, C. S. Robison, M. A. Whitt, and T. Miyamura.** 2001. Characterization of pseudotype VSV possessing HCV envelope proteins. Virology **286:**263–275.
27. **Matsuyama, S., M. Ujike, S. Morikawa, M. Tashiro, and F. Taguchi.** 2005. Protease-mediated enhancement of severe acute respiratory syndrome coronavirus infection. Proc. Natl. Acad. Sci. USA **102:**12543–12547.
28. **Qiu, Z., S. T. Hingley, G. Simmons, C. Yu, J. Das Sarma, P. Bates, and S. R. Weiss.** 2006. Endosomal proteolysis by cathepsins is necessary for murine coronavirus mouse hepatitis virus type 2 spike-mediated entry. J. Virol. **80:**5768–5776.
29. **Rota, P. A., M. S. Oberste, S. S. Monroe, W. A. Nix, R. Campagnoli, J. P. Icenogle, S. Penaranda, B. Bankamp, K. Maher, M. H. Chen, S. Tong, A. Tamin, L. Lowe, M. Frace, J. L. DeRisi, Q. Chen, D. Wang, D. D. Erdman, T. C. Peret, C. Burns, T. G. Ksiazek, P. E. Rollin, A. Sanchez, S. Liffick, B. Holloway, J. Limor, K. McCaustland, M. Olsen-Rasmussen, R. Fouchier, S. Gunther, A. D. Osterhaus, C. Drosten, M. A. Pallansch, L. J. Anderson, and W. J. Bellini.** 2003. Characterization of a novel coronavirus associated with severe acute respiratory syndrome. Science **300:**1394–1399.
30. **Sainz, B., Jr., J. M. Rausch, W. R. Gallaher, R. F. Garry, and W. C. Wimley.** 2005. Identification and characterization of the putative fusion peptide of the severe acute respiratory syndrome-associated coronavirus spike protein. J. Virol. **79:**7195–7206.
31. **Schmidt, O. W., and G. E. Kenny.** 1982. Polypeptide and functions of antigens from coronavirus 229E and OC43. Infect. Immun. **35:**515–522.
32. **Simmons, G., J. D. Reeves, A. J. Rennekamp, S. M. Amberg, A. J. Piefer, and P. Bates.** 2004. Characterization of severe acute respiratory syndrome-associated coronavirus (SARS-CoV) spike glycoprotein-mediated viral entry. Proc. Natl. Acad. Sci. USA **101:**4240–4245.
33. **Simmons, G., D. N. Gosalia, A. J. Rennekamp, J. D. Reeves, S. L. Diamond, and P. Bates.** 2005. Inhibitors of cathepsin L prevent severe acute respiratory syndrome coronavirus entry. Proc. Natl. Acad. Sci. USA **102:**11876–11881.
34. **Snijder, E. J., P. J. Bredenbeek, J. C. Dobbe, V. Thiel, J. Ziebuhr, L. L. Poon, Y. Guan, M. Rozanov, W. J. Spaan, and A. E. Gorbalenya.** 2003. Unique and conserved features of genome and proteome of SARS-coronavirus, an early split-off from the coronavirus group 2 lineage. J. Mol. Biol. **331:**991–1004.
35. **Song, H. C., M. Y. Seo, K. Stadler, B. J. Yoo, Q. L. Choo, S. R. Coates, Y. Uematsu, T. Harada, C. E. Greer, J. M. Polo, P. Pileri, M. Eickmann, R. Rappuoli, S. Abrignani, M. Houghton, and J. H. Han.** 2004. Synthesis and characterization of a native, oligomeric form of recombinant severe acute respiratory syndrome coronavirus spike glycoprotein. J. Virol. **78:**10328–10335.
36. **Sturman, L. S., C. S. Richard, and K. V. Holmes.** 1985. Proteolytic cleavage of the E2 glycoprotein of murine coronavirus: activation of cell-fusing activ-

ity of virions by trypsin and separation of two different 90K cleavage fragment. J. Virol. **56**:904–911.
37. **Taguchi, F., and Y. K. Shimazaki.** 2000. Functional analysis of an epitope in the S2 subunit of the murine coronavirus spike protein: involvement in fusion activity. J. Gen. Virol. **81**:2867–2871.
38. **Ujike, M., H. Nishikawa, A. Otaka, N. Yamamoto, N. Yamamoto, M. Matsuoka, E. Kodama, N. Fujii, and F. Taguchi.** 2008. Heptad repeat-derived peptides block the protease-mediated direct entry from cell surface of SARS coronavirus but not entry via endosomal pathway. J. Virol. **82**:588–592.
39. **Weiss, S. R., and S. Navas-Martin.** 2005. Coronavirus pathogenesis and the emerging pathogen severe acute respiratory syndrome coronavirus. Microbiol. Mol. Biol. Rev. **69**:635–664.
40. **Xiao, X., S. Chakraborti, A. S. Dimitrov, K. Gramatikoff, and D. S. Dimitrov.** 2003. The SARS-CoV S glycoprotein: expression and functional characterization. Biochem. Biophys. Res. Commun. **312**:1159–1164.
41. **Yamada, Y. K., K. Takimoto, M. Yabe, and F. Taguchi.** 1997. Acquired fusion activity of a murine coronavirus MHV-2 variant with mutations in the proteolytic cleavage site and the signal sequence of the S protein. Virology **227**:215–219.

Exp. Anim. 57(4), 357–365, 2008

Detection of the Antibody to Lymphocytic Choriomeningitis Virus in Sera of Laboratory Rodents Infected with Viruses of Laboratory and Newly Isolated Strains by ELISA Using Purified Recombinant Nucleoprotein

Kazuhiro TAKIMOTO[1)], Motoko TAHARAGUCHI[1)], Shigeru MORIKAWA[2)], Fumio IKE[3)], and Yasuko K. YAMADA[1)]

[1)]*Division of Experimental Animal Research and* [2)]*Department of Virology I, National Institute of Infectious Diseases, 1–23–1 Toyama, Shinjuku-ku, Tokyo 162-8640, and* [3)]*RIKEN BioResource Center, 3–1–1 Koyadai, Tsukuba-shi, Ibaraki 305-0074, Japan*

Abstract: *An enzyme-linked immunosorbent assay (ELISA) was developed to detect the antibody against lymphocytic choriomeningitis virus (LCMV) in sera of laboratory animals. In this ELISA system, LCMV-nucleoprotein (NP) expressed by recombinant baculovirus and purified with high molar urea was used as the antigen. Sera from laboratory animals experimentally infected with the Armstrong strain or the newly isolated M1 strain of LCMV were examined to detect anti-LCMV antibody by the ELISA system, and the reactivity was compared with that of IFA test. Regardless of LCMV strain, all the sera of adult mice infected with LCMV were positive with very high optical density (OD). Also, the sera from mice neonatally infected with LCMV M1 strain were positive with slightly lower OD than adult mice. In contrast, all the sera of uninfected mice were negative to LCMV-NP antigen. Similarly, anti-LCMV antibodies were detected in all the sera of hamsters, mastomyses, and gerbils infected with the LCMV Armstrong strain. The results of the ELISA were in complete agreement with those of IFA, and indicate the high sensitivity and specificity of the ELISA system in the detection of anti-LCMV antibody. Because this ELISA system does not require handling infectious LCMV in the course of the antigen preparation and serological assay, there is no risk of contamination in the laboratory or nearby animal facility. In addition, by using negative control antigen in parallel with positive antigen in ELISA, we can exactly check the LCMV contamination in laboratory animals.*

Key words: *baculovirus, ELISA, laboratory rodent, lymphocytic choriomeningitis virus, recombinant nucleoprotein*

Introduction

Lymphocytic choriomeningitis virus (LCMV) is an RNA arenavirus and an important zoonotic pathogen. Although humans infected with LCMV commonly have no symptoms or experience only mild febrile illnesses, patients suffer aseptic meningitis in severe cases. House mice (*Mus musculus*) are the natural hosts of LCMV and

(Received 5 October 2007 / Accepted 17 December 2007)

Address corresponding: K. Takimoto, Division of Experimental Animal Research, National Institute of Infectious Diseases, 1–23–1 Toyama, Shinjuku-ku, Tokyo 162-8640, Japan

transmit the virus to same and/or other species including humans [16]. Hamsters are also known to be susceptible to LCMV and are a potential source of prevalence of LCMV [17]. When LCMV infects immunocompetent adult mice, the virus is eliminated by the host immune response. However, if mice are infected with LCMV in utero or in the neonatal period, the virus infects persistently without marked clinical signs until immune complex glomerulonephritis occurs at 7–10 months of age [9]. In such mice, infectious virus is permanently excreted in the urine, saliva, and milk [16]. From investigations of antibody against LCMV, wild house mice are commonly contaminated with LCMV on a global basis [4, 13, 15]. These mice become natural reservoirs and could transmit LCMV to laboratory animals [20]. Other than wild mice, the main source of LCMV infection in laboratory animals is transplantation of tumors contaminated with LCMV. Several cases have been reported in which laboratory workers were accidentally infected with LCMV by contact with laboratory mice and Syrian hamsters implanted with tumors infected with LCMV [1, 6, 7]. Outside the laboratory, LCMV outbreaks have occurred among humans associated with pet hamsters [2].

In Japan, LCMV was first isolated from laboratory mice and guinea pigs in 1937 [11]. Sato and Miyata [18] reported that the antibody against LCMV was detected in laboratory animals in a survey of animal facilities in 1986. It has been the only report to suggest the possibility of LCMV infection in laboratory animals in Japan for decades after the first isolation of LCMV. Recently, in 2005, LCMV contamination was found in a wild-derived mouse strain imported from the Institut Pasteur (Paris, France) to RIKEN BioResource Center (Tsukuba, Japan) [10]. This case reminds us that LCMV contamination should be monitored even though the contamination rarely occurs in Japan.

Since LCMV is a zoonotic pathogen, it is better not to use live LCMV in the monitoring system. Using a recombinant expressing system can reduce the risk of treating infectious virus. In this study, we confirmed that our ELISA system using recombinant LCMV-nucleoprotein (NP) antigen worked well for detecting anti-LCMV antibody. Using this system, we determined whether antibody from mice experimentally infected with a recently isolated LCMV strain cross-reacted to the recombinant antigen made from a well-documented laboratory strain of LCMV, since there is the possibility of antigenic variation among LCMV strains. We also determined antibody reactivity of sera from mice experimentally infected in the neonatal period, because it was reported that mice become tolerant to LCMV when they are infected in this period. The results show that our ELISA system was sensitive enough to detect the newly isolated strain including neonatal infection.

As well as mouse species, other rodents such as hamsters, gerbils (*Meriones unguiculatus*), mastomyses (*Praomys coucha*), etc., are used as laboratory animals. Although hamsters are well known to have the potential of being a LCMV reservoir, as described above, the susceptibility of gerbils and mastomyses to LCMV has not previously been investigated. Considering the wide range of hosts of LCMV, the risk of LCMV contamination from gerbils and mastomyses cannot be denied. In this study, we tried to detect anti-LCMV antibody in laboratory rodents including gerbils and mastomyses.

Materials and Methods

Animals

Specific-pathogen-free (SPF) mice, gerbils, mastomyses, and hamsters were used for experimental infection with LCMV. Female C57BL/6CrSlc (6 weeks of age), C3H/HeSlc (6 weeks and pregnant), and Slc:ICR (4 weeks) mice were obtained from Japan SLC Inc. (Hamamatsu, Japan). The ICR mice were maintained for several months and used as sentinel animals in routine microbiological monitoring in our facility. The sera from ICR mice were used as negative control samples. Female gerbils (MON/JmsGbsSlc) (6 weeks) were obtained from Japan SLC Inc.; male mastomyses (MCC) (4 weeks) and male hamsters (HAW) (12 weeks) maintained in our facility were used for experimental infection. Sera used for negative control were obtained from the following animals maintained in our facility: a female gerbil (Mg-W) (24 weeks), female gerbils (Mg-B) (24 and 48 weeks), male and female mastomyses (MCC) (20 weeks), and female hamsters (HAW) (14, 16, and 38 weeks).

All the animals were nursed under barrier conditions and provided with water and commercial laboratory mouse chow *ad libitum*. Animal experiments were con-

ducted in accordance with "Guides for animal experiments performed at NIID".

Viruses

Recombinant baculovirus, which was inserted the coding region of the gene for the nucleoprotein of LCMV WE strain using the transfer vector pAcYM1 [14], and polyhedrin-deleted baculovirus, which was constructed by co-transfection of baculovirus DNA and pAcYM1 with no coding region of the gene, were kindly provided by Dr. Matsuura (Research Institute for Microbial Diseases, Osaka University). Baculoviruses were propagated in Tn5 cells and virus titers were determined by the 50% tissue culture infectious dose method.

The Armstrong strain and the M1 strain of LCMV were used for experimental infection. The M1 strain was isolated from wild-derived MAI/Pas mice persistently infected with LCMV which were imported from France and bred at RIKEN BioResource Center (Japan) [10]. Both strains of LCMV were propagated in Vero E6 cells and virus titers were measured by counting the number of infected cell foci detected by the peroxidase-anti-peroxidase method (PAP method) as previously described [21].

Preparation of LCMV-NP antigen

LCMV-NP antigen was prepared from Tn5 cells infected with the recombinant baculovirus expressing LCMV-NP at a multiplicity of infection (MOI) of 0.2. At 3 days post-infection, the cells were harvested and washed three times with PBS. The cells were resuspended in 1% NP40/PBS, allowed to stand on ice for 15 min, and centrifuged at 10,000 rpm for 10 min. The pellet was serially treated with urea solutions at different concentrations. First, the pellet was suspended in 1 M urea in 1% NP40/PBS, sonicated, and centrifuged at 8,000 rpm for 5 min. Then, the pellet was washed in PBS and suspended in 2 M urea in PBS. After the suspension was sonicated and centrifuged, the pellet was washed in PBS and suspended in 8 M urea in PBS. The suspension was sonicated and centrifuged, and the supernatant was used as LCMV-NP antigen. Negative control antigen was prepared likewise from Tn5 cells infected with polyhedrin-deleted baculovirus. To prepare crude LCMV-NP antigen, the infected Tn5 cells were resuspended in PBS and sonicated on ice three times for 20 sec according to the method of Homberger *et al.* [8]. The resulting cell extract was used as crude LCMV-NP antigen. Crude negative control antigen was prepared likewise from Tn5 cells infected with polyhedrin-deleted baculovirus. The protein concentration of antigens was determined by using a commercial kit, Bradford protein assay (Bio-Rad Laboratories, Hercules, CA). To assess the quality of purified antigens, an aliquot of antigens was electrophoresed on 10% SDS-PAGE gel and stained with Coomassie blue solution containing 0.1% Coomassie Brilliant Blue R-250, 30% methanol and 10% acetic acid.

LCMV infection

C57BL/6 mice and mastomyses were infected with 1×10^5 focus forming units (FFU) of the Armstrong strain of LCMV in PBS, intraperitoneally. Similarly, gerbils and hamsters were infected with 1.7×10^5 FFU and 2.5×10^5 FFU of the Armstrong strain of LCMV, respectively. At 4 weeks post infection, the animals were anesthetized with isoflurane, and sera were collected and kept at –80°C until use for antibody detection.

C3H/He mice were used to produce persistent LCMV carrier mice because neonates of C3H genetic background mice are highly susceptible to LCMV [5], and frequently used to produce LCMV carrier mice [22, 24]. Neonatal C3H/He mice obtained from pregnant mice were infected with 6.9×10^3 FFU of M1 strain of LCMV, intraperitoneally, within 18 h after birth. Adult C3H/He mice were also infected with 6.9×10^4 FFU of M1 strain of LCMV, intraperitoneally. The animals neonatally infected with LCMV at 6 or 8 weeks post infection and adult mice at 4 weeks post infection were anesthetized with isoflurane, and sera were collected and kept at –80°C.

Serological assays

Enzyme-linked immunosorbent assays (ELISA) were carried out using the LCMV-NP and negative control antigens prepared as above. The antigens were diluted 1:800 in 0.05 M carbonate-bicarbonate buffer (pH 9.6) and 100 μl was added to each well of a 96-well NUNC-immuno plate with a Polysoap surface (Nunc, Roskilde, Denmark). After incubation at 4°C overnight, the plate was washed three times with 0.05% Tween 20 in PBS (Tween-PBS). Then, the plate was blocked with 10% BlockAce (Dainippon Sumitomo Pharma, Osaka, Japan) in H_2O (blocking

buffer) for 1 h at room temperature and washed 3 times with Tween-PBS. In ELISA with crude LCMV-NP and negative control antigens, 3% gelatin in PBS was used for blocking [8]. One hundred microliters of sera diluted 1:100 in blocking buffer were added to LCMV-NP antigen and negative control antigen wells, incubated for 1 h at room temperature, and washed three times with Tween-PBS. Peroxidase-labeled goat anti-mouse IgG (Zymed Laboratories, San Francisco, CA), goat anti-hamster IgG (KPL, Inc., Gaithersburg, MD), or goat anti-rat IgG (Zymed) was diluted 1:4,000, 1:12,000, or 1:4,000, respectively, in blocking buffer, and 100 μl was added to each well. Since peroxidase-labeled anti-mastomys IgG and anti-gerbil IgG were not commercially available, both anti-mouse IgG and anti-rat IgG were alternatively used for the mastomys and gerbil systems. After the plate was incubated for 1 h at room temperature and washed three times with Tween-PBS, 100 μl of substrate solution consisting of 10 mg of *O*-phenylenediamine and 10 μl of H_2O_2 in 25 ml of 0.05 M phosphate-citrate buffer was added to each well and reacted in the dark for 30 min at room temperature. The reaction was stopped by adding 50 μl of 1 M H_2SO_4 and the chromogen produced was measured for absorbance at 492 nm.

To prepare the antigen for the immunofluorescence assay (IFA), Hela 299 cells were infected with the Armstrong strain of LCMV and incubated at 37°C in a 5% CO_2 atmosphere. After cytopathic effect was observed, the cells were harvested and mixed with equal numbers of uninfected Hela 299 cells. Then, about 1.3×10^4 cells in 10 μl PBS were spotted within printed circles of Teflon-coated glass slides (AR Brown, Tokyo, Japan) and air-dried with UV irradiation to inactivate LCMV for 2 h. After being washed with PBS, the cells were fixed with acetone for 10 min. The slides were stored at –80°C until use. Mouse sera diluted 1:100 or other animal species sera diluted 1:40 in PBS were applied to the IFA slides and incubated for 30 min at room temperature. Fluorescein isothiocyanate (FITC) -labeled anti-animal species IgGs were used as secondary antibodies. Rabbit anti-mouse IgG (Zymed) was used for the mouse, mastomys, and gerbil systems, and goat anti-hamster IgG (KPL) was used for the hamster system. The slides were reacted with the secondary antibodies for 30 min at room temperature and then examined under a fluorescence microscope.

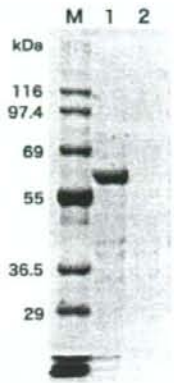

Fig. 1. SDS-PAGE analysis of purified recombinant proteins. Lane M, molecular weight marker proteins with the sizes indicated; lane 1, purified LCMV-NP antigen; lane 2, purified negative control antigen. A Protein band of LCMV-NP antigen, approximately 62 kDa (lane 1), was detected.

Results

We developed an ELISA system using recombinant LCMV-NP antigen purified with sequential urea treatment. The protein concentration was 0.7 mg/ml in purified LCMV-NP antigen, 0.6 mg/ml in purified negative control antigen, and 4.7 mg/ml in both crude LCMV-NP and negative control antigen. Purified LCMV-NP and negative control antigens were analyzed by SDS-PAGE. As shown in Fig. 1, LCMV-NP antigen was detected as a protein band at 62 kDa with 2 minor low molecular weight bands, which were also detected in negative control antigen. To confirm the usefulness of the ELISA system with purified antigen, anti-LCMV-NP antibody in the sera of four species of animals experimentally infected with LCMV was examined by the ELISA. In addition, the detection rate of anti-LCMV antibody of ELISA with purified antigen was compared to that of the IFA test, which is a well-established method for anti-LCMV antibody detection.

To determine the reactivity of mouse sera, adult C57BL/6 mice were infected with a laboratory strain (Armstrong) and adult or neonatal C3H/He mice were infected with the newly isolated M1 strain of LCMV.

Table 1. ELISA reactivity of sera from mice infected with LCMV

Mouse	LCMV strain infected[a]	Weeks post infection	No. of mice	ELISA titer (OD): Means ± SD (Range)			
				Purified antigen		Crude antigen	
				LCMV-NP	Negative control	LCMV-NP	Negative control
C57BL/6 (adult)	Armstrong	4	8	3.20 ± 0.12 (3.07–3.39)	0.20 ± 0.16 (0.12–0.59)	2.45 ± 0.18 (2.28–2.82)	0.44 ± 0.18 (0.17–0.72)
C3H/He (adult)	M1	4	8	3.02 ± 0.08 (2.90–3.14)	0.19 ± 0.13 (0.11–0.48)	2.89 ± 0.18 (2.56–3.11)	0.51 ± 0.19 (0.21–0.85)
C3H/He (neonate)	M1	6	4	2.05 ± 0.43 (1.61–2.50)	0.12 ± 0.04 (0.08–0.15)	2.48 ± 0.19 (2.41–2.72)	0.69 ± 0.29 (0.42–1.09)
C3H/He (neonate)	M1	8	5	2.45 ± 0.44 (2.06–3.18)	0.18 ± 0.14 (0.09–0.43)	2.84 ± 0.17 (2.64–3.11)	0.92 ± 0.53 (0.51–1.81)
ICR (adult)	Uninfected		20	0.08 ± 0.06 (0.02–0.30)	0.04 ± 0.04 (0.01–0.18)	nt[b]	nt

[a]Intraperitoneal inoculation. [b]Not tested.

Table 2. ELISA reactivity of sera from hamsters, mastomyses, and gerbils infected with LCMV

Animals[a]	LCMV strain infected[a]	No. of animals	Second antibody	ELISA titer (OD): Means ± SD (Range)	
				LCMV-NP antigen	Negative control antigen
Hamster	Armstrong	3	Anti-Hamster	1.98 ± 0.05 (1.94–2.04)	0.17 ± 0.06 (0.12–0.24)
Hamster	Uninfected	3	Anti-Hamster	0.21 ± 0.09 (0.13–0.30)	0.11 ± 0.05 (0.07–0.16)
Gerbil	Armstrong	2	Anti-Mouse	1.11 ± 0.46 (0.77–1.45)	0.03 ± 0.01 (0.03–0.05)
			Anti-Rat	2.60 ± 0.23 (2.43–2.77)	0.13 ± 0.05 (0.09–0.17)
Gerbil	Uninfected	3	Anti-Rat	0.21 ± 0.05 (0.17–0.27)	0.12 ± 0.02 (0.09–0.13)
Mastomys	Armstrong	4	Anti-Mouse	1.68 ± 0.19 (1.50–1.94)	0.03 ± 0.01 (0.02–0.04)
			Anti-Rat	1.87 ± 0.31 (1.57–2.23)	0.08 ± 0.03 (0.06–0.13)
Mastomys	Uninfected	4	Anti-Rat	0.12 ± 0.03 (0.09–0.15)	0.13 ± 0.05 (0.07–0.19)

[a]Four weeks post intraperitoneal inoculation.

Table 1 shows the anti-LCMV antibody detectability in the sera of mice in the ELISA test using recombinant LCMV-NP antigen or negative control antigen. In the mouse system, ELISA with crude LCMV-NP or negative control antigen was performed and the results were compared with those of ELISA with purified LCMV-NP or negative control antigen. In ELISA with purified antigens, regardless of the virus strains used, all the adult C57BL/6 and C3H/He mice infected with LCMV produced strong anti-LCMV antibody in the sera. Furthermore, C3H/He mice neonatally infected with LCMV M1 also produced strong anti-LCMV antibody in sera with slightly lower optical density (OD) than adult mice. In ELISA with negative control antigen, 1 of 8 adult C57BL/6 mice infected with the Armstrong strain, 1 of 8 C3H/He adult mice infected with the M1 strain, and 1 of 9 C3H/He mice infected neonatally with the M1 strain showed comparatively high OD, over 0.4. Since the OD values of these sera to LCMV-NP antigen were more than 5 times that to negative control antigen, it was clear that the responses were specific to the LCMV-NP antigen. On the other hand, 20 sera from ICR adult mice that were uninfected were LCMV-negative with low ELISA OD. In ELISA with crude LCMV-NP antigen, in all the mice infected with LCMV, anti-LCMV antibody was detected with OD similar to that in ELISA with purified antigen. However, in ELISA with crude negative control antigen, all the averages of OD were over 0.4 and 15 of 25 mice examined showed high OD, over 0.5.

The anti-LCMV antibody detectability of other animal species is shown in Table 2. In the hamster system, anti-LCMV antibody was detected in all the sera of ham-

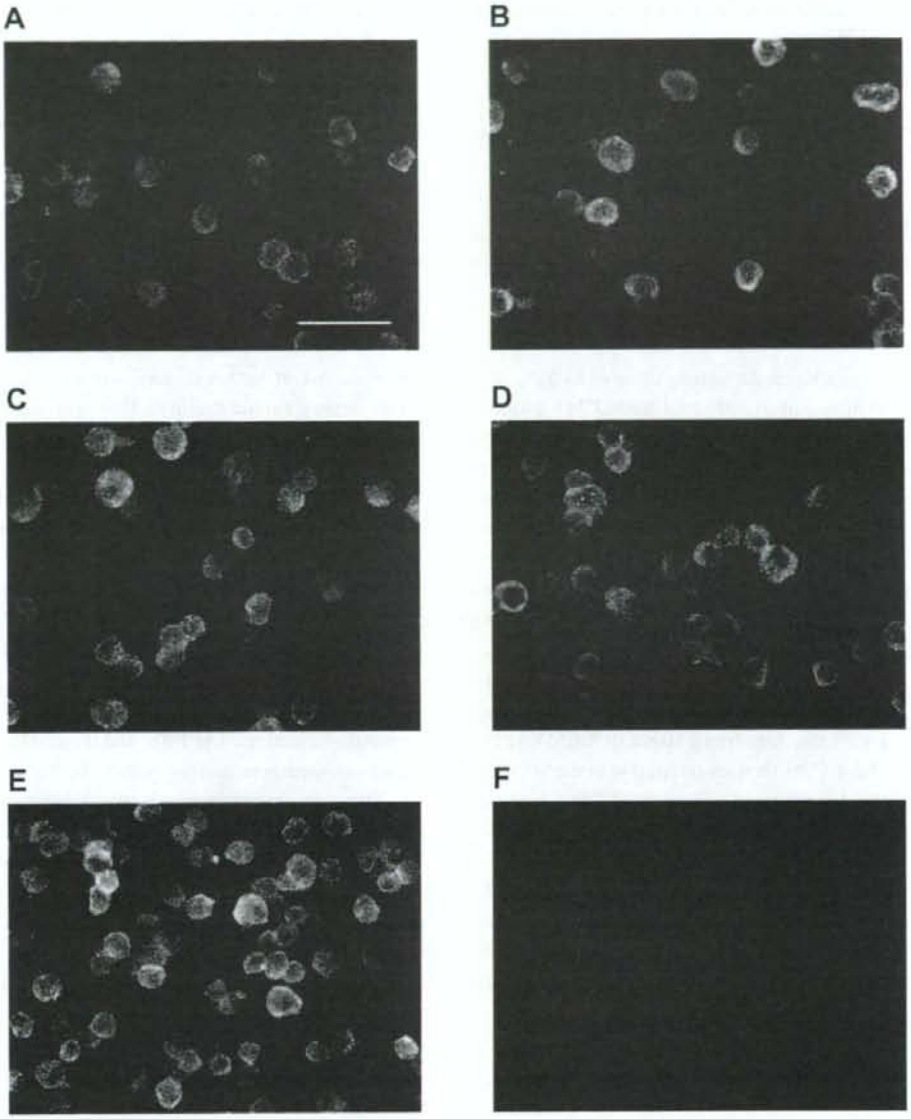

Fig. 2. IFA tests to detect the anti-LCMV antibodies in sera of each animal species. IFA slides were prepared using Hela 299 cells infected with the Armstrong strain of LCMV. Scale bar =50 μm. A to D represent the results of the Armstrong strain infected animal sera: A, mouse; B, hamster; C, mastomys; and D, gerbil. E represents the result of sera of adult mice at 4 weeks post infection with LCMV M1 strain. F represents the result of serum of negative control mouse.

Table 3. Comparison of ELISA and IFA results in examinations of sera from mice, hamsters, mastomyses, and gerbils infected with LCMV

Anti-LCMV Ab		Mouse				Hamster		Mastomys		Gerbil	
		Adult			Neonate						
IFA	ELISA	Armstrong[a]	M1	Uninfected	M1	Armstrong	Uninfected	Armstrong	Uninfected	Armstrong	Uninfected
Positive	Positive[b]	8	8	0	9	3	0	4	0	2	0
Positive	Negative	0	0	0	0	0	0	0	0	0	0
Negative	Positive	0	0	0	0	0	0	0	0	0	0
Negative	Negative	0	0	20	0	0	3	0	4	0	4

[a]Strain of LCMV, intraperitonael inoculation. [b]Value obtained by subtracting OD of negative control antigen from OD of LCMV-NP, higher than 0.5 is positive.

sters infected with the Armstrong strain of LCMV. Also in the sera of mastomys and gerbil, anti-LCMV antibody was detected using both anti-mouse IgG and anti-rat IgG secondary antibodies. In particular, anti-rat IgG secondary antibody showed a very strong reaction in the gerbil system. All animals showed very low OD to negative control antigen in the hamster, mastomys, and gerbil systems. In addition, uninfected sera from 3 hamsters, 4 mastomyses, and 3 gerbils were LCMV-negative with low ELISA OD.

In IFA tests, anti-LCMV antibody was clearly detected in all the sera obtained from the adult animals infected with the Armstrong strain of LCMV (Figs. 2A–D). Adult C3H/He mice infected with the M1 strain of LCMV also produced strong anti-LCMV antibody (Fig. 2E). In contrast, 20 sera of negative control mice were LCMV-negative in the IFA test (Fig. 2F).

Table 3 summarizes all the data described above. All the sera of animals infected with LCMV had LCMV-positive results in both ELISA and IFA tests, and the results of ELISA were in complete agreement with those of IFA (Table 3).

Discussion

In routine monitoring of laboratory animals, IFA and ELISA tests are usually used to detect anti-LCMV antibody [18–20]. For the IFA test, cells infected with LCMV are spotted onto glass slides as antigen [12, 18]. Also, it has been reported the antigen is prepared from cells infected with LCMV for the ELISA test [23]. Since these antigens are inactivated by acetone fixation, UV irradiation, or gamma irradiation before use for the test, there is no risk of further contamination in the laboratory or nearby animal facility. However, during the preparation of the antigen, handling of infectious LCMV is required, and it is necessary to treat LCMV in a biosafety containment facility. On the other hand, handling of recombinant LCMV-NP as an antigen, as reported in this paper, does not require the use of infectious LCMV in the course of the antigen preparation and serological assay.

ELISA with recombinant LCMV-NP has previously been reported by Homberger *et al.* [8]. In their paper, insect cells infected with recombinant baculovirus were harvested and sonicated in PBS, and the resulting cell extract was used as an antigen without further purification. Their antigen preparation method was very simple and the ELISA system was almost as sensitive as IFA. However, some sera of mice infected with LCMV, which were positive in IFA, were negative in ELISA. In our results using antigens prepared by the same methods, all the sera from mice infected with LCMV showed strong reactions in ELISA. However, there was also a comparatively strong reaction in ELISA with crude negative control antigen as shown in Table 1. These findings suggest that LCMV-positive serum might be judged to be LCMV-negative by screening using the ELISA system with crude antigens because of a high background level.

Recently, it was reported that LCMV contamination was not detected by ELISA using baculovirus recombinant LCMV-NP when the contamination occurred in Japan [10]. In our experience, antigen from baculovirus infected cells is not easily extracted. Therefore, in the present study, we used LCMV-NP obtained by purification with high molar urea as the antigen and this antigen

preparation seems to be more sensitive to anti-LCMV antibody than baculovirus recombinant LCMV-NP preparation without purification. In the detection of anti-LCMV antibody in the sera of animals experimentally infected with LCMV, all the sera were positive in both the IFA and ELISA tests and showed very high OD values in the ELISA test. On the other hand, most LCMV-positive sera showed very low OD values in ELISA with negative control antigen. In addition, all the sera of uninfected mice were negative in both the IFA and ELISA tests and showed very low OD values in the ELISA test. These findings indicate the high sensitivity and specificity of the ELISA system using purified antigen in the detection of anti-LCMV antibody.

A possibility still existed that the newly isolated M1 strain was not cross-reactive for recombinant LCMV-NP made from the laboratory strain. In our results, our antigen made from WE strain reacted well with sera infected with the newly isolated virus, showing our ELISA system is effective among LCMV strains. The usability of this system to detect antibody in natural infection should be examined in a further study.

It is well known that anti-LCMV antibody in serum of mice persistently infected with LCMV is difficult to detect because of their tolerance to LCMV. However, Buchmeier and Oldstone [3] showed the presence of antibodies against all LCMV structural peptides, even in mice neonatally infected with LCMV, and other investigators reported that anti-LCMV antibody was detected in the sera by double-sandwich ELISA with suspension of LCMV-carrier spleens as antigen [22]. In fact, in the present study, our recombinant antigen was able to detect anti-LCMV antibody in all the sera of mice neonatally infected with the M1 strain. Further investigation, examining sera of mice infected in utero with LCMV, is necessary to confirm whether our recombinant LCMV-NP antigen is useful for the detection of anti-LCMV antibody in mice infected with LCMV through vertical transmission.

The anti-LCMV antibody was detected in the sera from gerbils and mastomyses, suggesting that these animals are sensitive to LCMV. Although it is unknown whether or not these animals have the potential to be a reservoir of LCMV, it is desirable that these animals are periodically examined for LCMV contamination as well as mice and hamsters.

To exclude non-specific reactions of sample sera, it is useful that sera are reacted with negative control antigen in parallel with positive antigen in ELISA. In this study, Tn5 cells infected with polyhedrin-deleted baculovirus were used for the preparation of negative control antigen to exclude the reaction of serum to the materials derived from not only insect cells but also baculovirus. If an animal serum shows high antibody titer to LCMV-NP antigen, the reaction should be judged to be specific or non-specific to LCMV-NP antigen by comparison with the result of ELISA using the negative control antigen. Consequently, the precise LCMV specific antibody response can be obtained and hence we can accurately evaluate the LCMV contamination. Furthermore, the availability of this ELISA system for several laboratory rodents as demonstrated in this study suggests that this ELISA system is also available for the survey of wild rodents and humans outside the laboratory.

Recently, many laboratory mice are being transferred from overseas for research use. Due to the increase of the use of these mice, the possibility of LCMV contamination will be higher in the future. To prevent LCMV contamination in the facility, laboratory animals should be routinely examined by a sensitive and precise method to detect the antibody against LCMV in spite of the fact that LCMV has not been prevalent in Japan for many years.

References

1. Biggar, R.J., Schmidt, T.J., and Woodall, J.P. 1977. Lymphocytic choriomeningitis in laboratory personnel exposed to hamsters inadvertently infected with LCM virus. *J. Am. Vet. Med. Assoc.* 171: 829–832.
2. Biggar, R.J., Woodall, J.P., Walter, P.D., and Haughie, G.E. 1975. Lymphocytic choriomeningitis outbreak associated with pet hamsters. *JAMA* 232: 494–500.
3. Buchmeier, M.J. and Oldstone, M.B. 1978. Virus-induced immune complex disease: identification of specific viral antigens and antibodies deposited in complexes during chronic lymphocytic choriomeningitis virus infection. *J. Immunol.* 120: 1297–1304.
4. Childs, J.E., Glass, G.E., Korch, G.W., Ksizek, T.G., and Leduc, J.W. 1992. Lymphocytic choriomeningitis virus infection and house mouse (*Mus musculus*) distribution in Urban Baltimore. *Am. J. Trop. Med. Hyg.* 47: 27–34.
5. Doyle, L.B., Doyle, M.V., and Oldstone, M.B.A. 1980. Susceptibility of newborn mice with H-2^b backgrounds to

lymphocytic choriomeningitis virus infection. *Immunology* 40: 589–596.
6. Dykewicz, C.A., Dato, V.M., Fisher-Hoch, S.P., Howarth, M.V., Perez-Oronoz, G.I., Ostroff, S.M., Gary, H.Jr., Schonberger, L.B., and McCormick, J.B. 1992. Lymphocytic choriomeningitis outbreak associated with nude mice in a research institute. *JAMA* 267: 1349–1353.
7. Hinman, A.R., Fraser, D.W., Douglas, R.G., Bowen, G.S., Kraus, A.L., Winkler, W.G., and Rhodes, W.W. 1975. Outbreak of lymphocytic choriomeningitis virus infections in medical center personnel. *Am. J. Epidemiol.* 101: 103–110.
8. Homberger, F.R., Romano, T.P., Seiler, P., Hansen, G.M., and Smith, A.L. 1995. Enzyme-linked immunosorbent assay for detection of antibody to lymphocytic choriomeningitis virus in mouse sera, with recombinant nucleoprotein as antigen. *Lab. Anim. Sci.* 45: 493–496.
9. Hotchin, J. and Collins, D.N. 1964. Glomerulonephritis and late onset disease of mice following neonatal virus infection. *Nature* 203: 1357–1359.
10. Ike, F., Bourgade, F., Ohsawa, K., Sato, H., Morikawa, S., Saijo, M., Kurane, I., Takimoto, K., Yamada, Y.K., Jaubert, J., Berard, M., Nakata, H., Hiraiwa, N., Mekada, K., Takakura, A., Itoh, T., Obata, Y., Yoshiki, A., and Montagutelli, X. 2007. LCMV infection in a wild-derived mouse inbred strain undetected by dirty-bedding sentinel monitoring and revealed after embryo transfer of an inbred strain derived from wild mice. *Comp. Med.* 57: 272–281.
11. Kasahara, S., Hamano, R., Yamada, R., and Tsubaki, S. 1937. Choriomeningitis virus isolated in the course of experimental studies on epidemic encephalitis. *Trans. Soc. Pathol. Jpn.* 27: 581–585 (in Japanese).
12. Lewis, V.J., Walter, P.D., Thacker, W.L., and Winkler, W.G. 1975. Comparison of three tests for the serological diagnosis of lymphocytic choriomeningitis virus infection. *J. Clin. Microbiol.* 2: 193–197.
13. Lledó, L., Gegúndez, M.I., Saz, L.V., Bahamontes, N., and Beltrán, M. 2003. Lymphocytic choriomeningitis virus infection in a province of Spain: analysis of sera from the general population and wild rodents. *J. Med. Virol.* 70: 273–275.
14. Matsuura, Y., Possee, R.D., Overton, H.A., and Bishop, D.H.L. 1987. Baculovirus expression vectors: the requirements for high level expression of proteins, including glycoproteins. *J. Gen. Virol.* 68: 1233–1250.
15. Morita, C., Tsuchiya, K., Ueno, H., Muramatsu, Y., Kojimahara, A., Suzuki, H., Miyashita, N., Moriwaki, K., Jin, M.L., Wu, X.L., and Wang, F.S. 1996. Seroepidemilogical survey of lymphocytic choriomeningitis virus in wild house mice in China with particular reference to their subspecies. *Microbiol. Immunol.* 40: 313–315.
16. National Research Council. 1991. Infectious diseases of mice and rats. pp. 199–205. National Academy Press, Washington, D.C.
17. Parker, J.C., Igel, H.J., Reynolds, R.K., Lewis, A.M.Jr., and Rowe, W.P. 1976. Lymphocytic choriomeningitis virus infection in fetal, newborn, and young adult Syrian hamsters (*Mesocricetus auratus*). *Infect. Immun.* 13: 967–981.
18. Sato, H. and Miyata, H. 1986. Detection of lymphocytic choriomeningitis virus antibody in colonies of laboratory animals in Japan. *Exp. Anim.* 35: 189–192.
19. Schoondermark-van de Ven, E.M.E., Philipse-Bergmann, I.M.A., and Van der Logt, J.T.M. 2006. Prevalence of naturally occurring viral infections, *Mycoplasma pulmonis* and *Clostridium piliforme* in laboratory rodents in Western Europe screened from 2000 to 2003. *Lab. Anim.* 40: 137–143.
20. Smith, A.L., Paturzo, F.X., Gardner, E.P., Morgenstern, S., Cameron, G., and Wadley, H. 1984. Two epizootics of lymphocytic choriomeningitis virus occurring in laboratory mice despite intensive monitoring programs. *Can. J. Comp. Med.* 48: 335–337.
21. Tanishita, O., Takahashi, Y., Okuno, Y., Yamanishi, K., and Takahashi, M. 1984. Evaluation of focus reduction neutralization test with peroxidase-antiperoxidase staining technique for hemorrhagic fever with renal syndrome virus. *J. Clin. Microbiol.* 20: 1213–1215.
22. Thomsen, A.R., Vorkert, M., and Marker, O. 1985. Different isotype profiles of virus-specific antibodies in acute and persistent lymphocytic choriomeningitis virus infection in mice. *Immunology* 55: 213–223.
23. Turkovic, B. and Ljubicic, M. 1992. ELISA and indirect immunofluorescence in the diagnosis of LCM virus infections. *Acta Virol.* 36: 576–580.
24. Volkert, M., Bro-Jorgensen, K., Marker, O., Rubin, B., and Trier, L. 1975. The activity of T and B lymphocytes in immunity and tolerance to the lymphocytic choriomeningitis virus in mice. *Immunology* 29: 455–464.

J. Rakuno Gakuen Univ., 33 (1) : 139~150 (2008)

Gastroenteropathy in rodents with hepatic *Taenia taeniaeformis* larvae infection: mechanism of pathogenesis

Jose Trinipil LAGAPA[1,2], Yuzaburo OKU[3] and Masao KAMIYA[1]

(Accepted 24 July 2008)

Abstract

Parasites generally produce histopathological changes in organs or tissues of hosts where they are located. Hepatic *Taenia taeniaeformis* larvae infection in rodents, however, has been reported to induce gastric and intestinal hyperplasia despite the fact that the parasite is located remotely. This unique phenomenon suggested that in a host-parasite relationship, unforeseen pathological complications may occur in the infected host. Several mechanisms were hypothesized to influence gastroenteropathy in rodents during hepatic *T. taeniaeformis* larvae infections. Hypergastrinemia and immunosuppression were suggested to contribute to the development of lesions but recent studies showed inconsistencies of their association. More prominent among proposed geneses indicated factors from the larvae might cause this phenomenon. Excretory-secretory products of *T. taeniaeformis* larvae were proven to induce the hyperplastic lesions in the gastric mucosa of immunodeficient mice. Previous studies hinted that the larvae products were absorbed into the host's body and carried by the blood into the gastroenteric mucosa. Immunohistochemical studies have also supported the premise that the products were associated with hyperplastic lesions found from gastric to colonic mucosa of infected rodents. This review highlights the pathogenesis of gastroenteropathy during hepatic *T. taeniaeformis* larvae infection in rodents.

Introduction

In 1926, Johanes Fibiger won the only Nobel Prize for helminthology in inducing gastric cancer in rats by feeding them cockroaches infected with *Spiroptera neoplastica* (later renamed *Gongylonema neoplastica*) larvae. Although it was later criticized as not being true cancers, but merely worm-induced hyperplasia associated with vitamin A deficiency[40], it showed how parasites can produce lesions in their hosts. Generally, parasites produce histopathological changes in organs or tissues of hosts where they are located. In the case of parasites in liver, hepatic tissues and related organs suffer from either mechanical or immunological reactions. The pathologies are evoked by either the parasites or as hosts' responses against the invading organism. Likewise, in gastrointestinal parasitism, abnormalities are observed in specific sites of the digestive tract where the parasites are located. There are records, however, of parasite-free regions showing histological changes as a form of compensatory mechanism to incapacitated parasitized regions[20].

Hepatic *Taenia taeniaeformis* larvae infection in rats has been known to induce gastric and intestinal hyperplasia despite the fact that the parasite is located remotely in the liver[1,4,11,25,29,30,36,48]. This unforeseen consequence of pathology remote from the site of infection is a unique phenomenon in the aspect of parasitism. A dynamic and rapidly developing area of research in host-parasite relationship studies is

[1] Laboratory of Environmental Zoology, Department of Biosphere and Environmental Sciences, Faculty of Environment System, Rakuno Gakuen University, Bunkyodai-Midorimachi, Ebetsu, Hokkaido 069-8501, Japan
[2] College of Veterinary Medicine, Central Mindanao University, Musuan, Bukidnon, 8710, Philippines
[3] Laboratory of Parasitology, Department of Disease Control, Graduate School of, Hokkaido University, Kita 18, Nishi 9, Kita-ku, Sapporo 060-0818, Japan

the identification of immunomodulatory molecules from parasites[14]. On the other hand, increasing evidences of parasites causing cancer in hosts have been documented[40].

This review will highlight the different theories involved to explain the pathogenesis of *T. taeniaeformis* induced gastroenteropathy and aims to build on a greater understanding of the mechanism in the development of lesions. We presumed that a clearer grasp of this unique pathogenesis will advance knowledge of host-parasite relationships. Nevertheless, gaps are still apparent and need to be investigated towards full comprehension of this phenomenon and similar gastroenteropathies.

Parasitism and pathologies

Parasitism is a relationship of two organisms of different species in which the smaller (the parasite) has the potential of harming the larger (the host), and the parasite relies on the host for nutrient and for a place to live[38]. On one hand, since the parasite is dependent on its host, it is to its own advantage not to destroy the host. Although there are many species of parasites that are harmless to their host, there are also many forms that produce pathological changes and could lead to severe ill health or death of the host[59]. In order for a successful adaptation of the parasite in its host, it may induce conditions favourable for its own development and metabolism. Such favourable conditions could involve in maintaining an adequate body size and food supply, inducing immunosuppression and analgesia in the host, and influencing the speed of development of the host[58]. These mechanisms substantiated that there are effecter molecules secreted or excreted by some parasites that could cause unforeseen circumstances in host-parasite relationships.

To survive for long periods in a disadvantageous and aggressive environment, helminth parasites secrete several soluble factors that might interact with host cells and interfere cell to cell communications processes, thus would contribute into pathologic processes[17]. One classic example is the plerocercoids of Spirometrid tapeworms synthesizing and releasing plerocercoid growth factor that is transported by the blood, interacts with growth hormone receptors and mimics many of the biological actions of growth hormone[45].

Helminths such as *Schistosoma haematobium* and *Opisthorchis viverrini*, have been proven to be definitely carcinogenic to humans. Mechanisms of helminth-induced cancer are reported to include chronic inflammation, modulation of the host immune system, inhibition of intracellular communication, disruption of proliferation-antiproliferation pathways, induction of genomic instability and stimulation of malignant stem cell progeny[40].

Taenia taeniaeformis infection and gastroenteropathy in rodents

Taenia taeniaeformis is a tapeworm inhabiting the small intestine of the definitive hosts: cats and other carnivores. Gravid segments of the tapeworm containing the infective eggs are excreted with the hosts' feces. Rats, mice, and other wild rodents are known intermediate hosts and are infected by ingestion of the tapeworm eggs. These rodents harbour the hepatic dwelling larval stage, *Strobilocercus fasciolaris*. When infected rodents are preyed upon by susceptible carnivores, the larvae develop into tapeworm stage in the small intestine of definitive hosts to continue the life cycle of the parasite.

Bullock and Curtis[7,8] first observed "hepatic sarcomata" in chronically infected rats that was reported to disseminate throughout the abdominal cavity. "Hyperthropic gastritis" was described that caused the increase of stomach size in heavily parasitized rats[9]. Blumberg and Gardner[5] further described morphologically the increase of stomach size in heavily and chronically infected rats as more than double compared to the normal rat stomach.

After more than half a century, Cook and Williams[11] revisited the pathological changes in the stomach and small intestine by oral infection of rats with *T. taeniaeformis* eggs. This was followed by a parabiosis experiment that led to a hypothesis on the involvement of a chemical mediator or factors released by the larvae[12].

Investigation of gastroenteropathy in chronically infected rats up to 12 months of infection was made and found the lesions to intensify rather than subside[4]. An *in vitro* experiment on the effect of larval products on host gastric cells supported the hypothesis that factors from larvae are involved[49]. The same laboratory had demonstrated that larvae excretory-secretory products were located in the cytoplasm of hyperplastic cells by immunoperoxidase staining[50]. Further investigation on larval products was made by intraperitoneal implantation of larvae into rats inducing gastropathy[26].

It was also reported that the neutral mucous cell was the major type of hyperplastic mucous cells observed[48]. Electron microscopic studies were done in hyperplastic cells and suggested undifferentiated cells as the primary proliferating cells[25].

The effect of gastrin and gastric alkalinity was also indicated as a secondary factor in the development of lesions. It was confirmed also that there is a concomitant occurrence of gastric hyperplasia, hypergastrinemia, and intragastric alkalinity[1].

Immune down regulation during the course of infection facilitating the hyperplastic stimulus and earlier occurrence of gastropathy in immune deficient rats was suggested[2]. Using severe combined immune-deficient (SCID) mouse as animal model, oral, intraperitoneal and subcutaneous inoculation of *T. taeniaeformis* eggs or *in vitro*-hatched oncospheres and larvae implantation resulted in various degrees of gastropathies[27].

Gastroenteropathy is described grossly as significant enlargement of the stomach and small intestine. Excessive mucus productions with focal lesions of white plaques or nodules were observed in gastric mucosa. The most common visible lesion observed was of diffuse nodular mucosal thickening of the gastric inner wall. The mucosa of the small intestine was also thickened particularly in the duodenum and proximal jejunum with mucoid intestinal contents. Recent study observed colonic mucosa appearing edematous as well.

Microscopically, the gastric mucosal length was markedly increased and normal structure of gastric units composed of the pit, isthmus, neck and the base could not be identified. Mucosal hyperplasia is characterized by Periodic acid-Schiff reaction (PAS) and PAS-alcian blue (PAB) positive cells as responsible for multi-fold increases in height of gastric units. Konno et al.,[25] observed by electron microscopy that features of these cells were immature-like mucous cells. These cells were observed to be pit or neck mucous precursor cells occupying dilated gastric glands. Numerous cystic cavities were also found filled with PAB-positive mucus. Significant loss in the number of parietal and zymogenic cells in the gastric mucosa was observed[29]. Patchy infiltration of mononuclear cells and eosinophils were also seen[11].

Small intestinal changes comprised up to 2-fold increases in villus and crypt lengths but there was no significant changes observed in epithelial cell numbers. In chronic infection, distortion of normal architecture of the mucosa was observed due to the accumulation of mucus and subsequent dilation of the crypts. These dilatations contained a mixture of strongly PAS-positive mucus, sloughed epithelial cells and pyknotic nuclear fragments, which often become calcified. Intestinal mast cell and eosinophil counts were observed to have increased in number. Recent studies in rats also showed a 2-fold increase of mucosal cell number in the duodenum[29].

Present results showed mucosal length of colon increasing up to 3-4 folds with goblet cell number significantly greater than the control. Few cystic dilatations were found similar to the small intestines.

Pathogenesis of gastroenteropathy during hepatic *T. taeniaeformis* larvae infection

Taenia taeniaeformis *larvae excretory-secretory products*

Involvement of either chemical mediators or excretory-secretory products of *T. taeniaeformis* larvae had been suggested as the primary cause for inducing gastric hyperplasia in infected rats. Cook et al.,[11] first postulated that larvae derived

chemicals/factors transported by blood circulation are involved because an uninfected rat joined surgically to a heavily infected partner by parabiosis showed gastroenteropathy. Excretory-secretory products of larvae were reported to stimulate growth of host gastric cells *in vitro*[49], and were observed to be concentrated in specific areas of the cytoplasm of hyperplastic stomach epithelial cells[50]. This observation prompted Blaies and Williams[4] to attempt inducing gastric hyperplasia in rats by larval implantation of 40 larvae and intraperitoneal injection of TtLES (*T. taeniaeformis* larvae excretory-secretory) product into rats. Although the result was a failure, a follow up study increasing the number of larvae implanted (150-300) into the peritoneal cavity of rats induced gastric hyperplasia[26]. This finding suggested that the volume of excretory-secretory product played an important role.

Using severe compromised immune-deficient mouse proved that inoculation forms of parasites and routes of infection influenced larval development and affected initiation of gastric hyperplasia[27]. Inoculation of either parasite egg or oncospheres was preferably by oral route because it facilitated the infection into the organ of predilection (liver). Similarly, intraperitoneally inoculated *in vitro*-hatched oncospheres that were able to penetrate the liver of SCID mice also grew faster than those inhabiting the peritoneal cavity. Apparently, the development of larvae was faster in the liver than in other sites of infection.

The common denominator of all these factors —— the inoculation form of parasite and route of infection —— rests upon which produced the greater number of large sized larvae that resulted to gastroenteropathy. Induced gastric hyperplasia is suggested as being dependent on the number and size of larval cysts. The volume of excretory-secretory products apparently was relative to the size and number of larvae[26,48].

A significant correlation was observed between increase of stomach weight in infected rats and the number of hepatic larvae in rats at 12-20 weeks post-inoculation[48]. Increasing the number of implanted larvae into rats induced hyperplastic lesion. Inoculated SCID mice revealed that the degree of gastric hyperplasia was dependent on number and size of developed larvae[27]. This correlated to recent observations that *in-vitro* culture of 9-week old larvae produces lesser gram of protein per larvae than larger 12-week old larvae. Furthermore, daily injection of 1 mg protein/day resulted to gastric mucous pit cell hyperplasia and decrease in parietal cell number at 1 WPI while those injected with 0.5 mg protein /day did not show significant changes in gastric mucosa until 4 WPI[28]. These findings proved that volume of the TtLES product is an important factor in the development of gastric hyperplasia.

Hammerberg and Williams[16] reported that *T. taeniaeformis* larval *in vitro* products contained polysulfated glycosaminoglycan. These molecules have been detected on surfaces of various infectious organisms. Glycosaminoglycans were suggested as playing a role in the healing process of acetic acid ulcer in rat stomach[60]. Parasitic glycosaminoglycans were suggested to stimulate the growth of gastric epithelial cells[49].

Gastroenteropathy and immunity

Immunity was observed to be a factor that influences length of pre-patent period (period from inoculation until development of gastric hyperplasia). Eventual down regulation of host immune response during the course of infection presumably by larval proteinase inhibitor was suggested[2]. Immune response of host once inhibited may facilitate the action of TtLES product. Infected athymic nude rats developed gastric hyperplasia earlier than euthymic rats that implicated T cell mediated response as involved. Immunodeficient mice lacking T cell responses also developed gastric hyperplasia sooner than immunocompetent ones. On the other hand, T cell dependent cell mediated responses were noted in resistance to *T. taeniaeformis* infection as early as 5 days post infection[21]. Collating these results would indicate that T cell responses affect establishment and might inhibit growth of larvae, to which the volume of TtLES product was dependent. T cell immune response therefore is suggested to affect gastric hyperplasia indirectly by

its action on development of larvae.

A study had suggested the possibility that locally produced inflammatory and T cell derived cytokines could facilitate hyperplastic changes[62]. To the contrary, development of gastropathy in *T. taeniaeformis* infection was observed earlier in athymic nude rats in the absence of T cell-mediated responses over immunocompetent rats[2]. Later occurrence of gastropathy in immune competent rats might have suggested the role of T cell immune response in resistance to *T. taeniaeformis* infection[21], that may have an effect on the establishment and growth of larvae. *T. taeniaeformis* induced gastric hyperplasia in SCID mice lacking any T cell-mediated responses[6] further supported these observations. Larval cyst size and number are found to be very important factors in inducing the hyperplastic lesions as revealed by these results.

Hypergastrinemia and increase of intragastric pH

The implication of gastrin in pathogenesis of gastric hyperplasia was suspected since this hormone exerts trophic effects on gastrointestinal tissues[63]. Serum gastrin concentration in rats infected with larval *T. taeniaeformis* was remarkably reaching up to 100-fold increase[12]. However, the same authors reported that antrectomized rats developed also gastric hyperplasia without elevation of serum gastrin levels. Abella et al.,[1] noted that there was simultaneous and abrupt occurrence of gastric hyperplasia, hypergastrinemia, and rise in intragastric pH in infected rats without prior alterations on these parameters. Further observations in chronic gastric hyperplasia for 1 year or more revealed that gastrin levels returned to normal level whereas the stomach was enormously enlarged. These findings suggested that occurrence of hypergastrinemia is secondary to gastric hyperplasia. It was also suggested that increase secretion of mucus by mucous cells leads to the rise of intragastric pH that resulted to hypergastrinemia[26].

On the other hand, loss of parietal cells had been consistently observed in hyperplastic mucosa. Loss of functional numbers of parietal cells was suggested to be due to preferential differentiation of stem cells to mucus-producing cells and pressure atrophy resulting from uncontrolled growth of surrounding cells[1]. SCID mice intraperitoneally inoculated with *in vitro*-hatched oncospheres were observed to have noticeable decrease in parietal cell number along with minimal increase in immature and mucous pit cell number at 2 WPI. Taking into account this result, it is conceivable that signs of parietal ablation could have occurred earlier than the concomitant onset of gastric mucosal hyperplasia, rise of intragastric pH and hypergastrinemia.

Parietal and zymogenic cells loss

Parietal cell loss was mentioned as probable cause in rise of intragastric pH and hypergastrinemia. Parietal cell loss was observed to be associated with the degree of mucosal cell hyperplasia. Significant loss of parietal cells in various degree of hyperplasia in SCID mice models corroborated with reports associating parietal cell loss with the development of characteristic changes of mucosal cell hyperplasia[28]. The mechanism of the loss of parietal cells in this phenomenon is unknown.

Extensive studies disclosed that nematode parasites inhabiting the stomach of mammalian animals have the ability to inhibit acid secretion causing increases in gastrin secretion[57]. Acid is generated in parietal cells in fundic region by proton pump. Abomasal nematodes may cause dysfunction or loss of parietal cells by blocking the proton pump or interfere with the complex pysiological regulation of the parietal cells[53]. Dysfunction and loss of parietal cells decreases acid secretion and cause the increase of pH in stomach. Removal of acid feedback in turn would cause hypergastrinemia in parasitized animals[31]. However, no concrete evidence yet can be shown that indeed parietal cell loss occurred prior to the rise of intragastric pH in *T. taeniaeformis*-induced gastric hyperplasia.

Reduction in the number of parietal cells during gastric hyperplasia in sheep transplanted with